Contrib. Astron. Obs. Skalnaté Pleso **53/1**, 28 – 45, (2023)
https://doi.org/10.31577/caosp.2023.53.1.28

Appropriate site selection for the astronomical observatory - Erzincan province sample application

A. Yılmaz

Health Services Vocational School, Erzincan Binali Yıldırım University, Erzincan, Turkey (E-mail: abdulvahap.yilmaz@erzincan.edu.tr)

Received: January 26, 2023; Accepted: March 20, 2023

Abstract. In this study, remote sensing methods, a multicriteria decision analysis, and the GIS program were used to determine the most suitable sites for the construction of an astronomical observatory. The study was conducted within the provincial boundaries of Erzincan, where there is not yet an observatory. The study identified and analyzed meteorological, geographic and anthropogenic factors (cloud cover, precipitable water, wind speed, geology and landslides, active fault lines, digital elevation model, urban lighting, mining activities, distance to roads). The areas proposed as a result of the study were plotted on the city map. It is important to reduce the number of eligible areas to be site tested by performing the work prior to the site testing phase, which is one of the phases required for the construction of the observatory. This study will provide energy, time, and cost savings by reducing the number of alternative areas. As a result of the preliminary study we conducted to select the most suitable site for the observatory, the final decision should be made after the proposed areas have been subjected to the site test phases.

Key words: Site selection – Astronomical observatory – Multi-Criteria Decision Analysis – AHP – GIS

1. Introduction

In order for observatories to operate at high efficiency, it is important that the site where they are built provide the most ideal observing conditions. Site selection is an evaluation process to create the most suitable conditions by combining many elements from different sources and consists of the steps of site selection and site testing, Hudson & Simstad (2010) and Koc-San et al. (2013). Site testing is a process that requires many steps, such as sky brightness, atmospheric visibility, precipitable water vapor, and atmospheric extinction coefficient calculation Koc-San et al. (2013). This process will expand in direct proportion to the number of alternatives. It is important to select the site in such a way that the number of alternatives is limited in order to reduce the time, energy, and

cost required for the site testing process. The use of multi-criteria decision analysis (MCDA) in conjunction with geographic information systems (GIS) and remote sensing, and the ability to manage complex and voluminous data from multiple data sources, is a powerful tool that provides an efficient process for site selection. In recent years, the development of remote sensing resources for site selection, the use of MCDA and AHP, and their support by a GIS system have attracted the attention of researchers, Koc-San et al. (2013). The Analytic Hierarchy Process (AHP) has become one of the most widely used methods in the decision analysis since its development by Saaty (1988). AHP is a method of decision making in which the weights of criteria are determined by pairwise comparisons. The determination of weights by expert decision makers who evaluate the criteria increases the reliability of the method. There are many studies in various fields using decision analysis approaches along with GIS, AHP and the multi-criteria decision analysis (MCDA). Selection of the most suitable site for a biogas plant, Tulun et al. (2022), selection of sites for solid waste disposal Bilgilioglu et al. (2022), collection areas after earthquakes, Aman & Aytac (2022). The first site selection for an astronomical observatory in Turkey was made in 1989 by Aslan et al. when determining the site for the construction of the TUeBTAK National Observatory (TUG). In this study, field experiments, meteorological measurements and anthropogenic factors were given priority in determining the suitable site, Koc-San et al. (2013). Another study was conducted in 2013 by Koc-San Vd. using GIS, the MCDA method integrated with remote sensing methods and AHP to propose alternative sites for the TUeBTAK National Observatory. The importance of astronomy in the world the increasing growth of Erzincan Binali Yıldırım universty in Erzincan Province, the prediction of scientific studies in the field of astronomy in the future encouraged us to choose the appropriate place for the construction of an observatory within the boundaries of the province. The aim of our study is to identify the most suitable sites for the construction of an observatory in the province. A method combining MCDA with remote sensing technologies and geographic information systems (GIS) was used to select the suitable site, Koc-San et al. (2013). There are many parameters to be considered when selecting an astronomical observatory with the most efficient operating conditions, Jia et al. (2012). Important parameters affecting the selection of suitable sites for astronomical observatories have been published by Walker (1984), Cowles (1989) and Hudson & Simstad (2010). In addition, a study similar to our study was conducted for Antalya province. Considering these studies, the parameters affecting the selection of a suitable site for the observatory were determined by Koc-San et al. (2013). In this study, three main groups were formed as meteorological, geographical, and anthropogenic parameters, 10 factors were created among these main groups and recorded as grid layers in GIS, Koc-San et al. (2013). According to the AHP method, these layers were compared with each other and their weighting values were determined by the experts. Considering these weighting values, the most suitable site was selected for the astronomical observatory in Erzincan, Turkey. In this study, we

propose the most suitable optical astronomical observatory for construction by mainly overlapping the maps that we created by digitizing in the system GIS as a result of the data analysis using remote sensing, MCDA and AHP methods for site selection.

2. Workspace and data used

The study area is located in the western part of the Eastern Anatolian region of Erzincan province in Turkey and covers 11.815 km^2, Figure 1. From the data of the General Directorate of State Meteorological Affairs of Erzincan Province, the average number of clear days per year is 116.6. In winter, when the air mass coming from Siberia acts from the east, there may be very severe winter days. The average annual temperature in Erzincan is 10.9 C, with an average of -6.7 C in January, the coldest month, and an average of 31.4 C in July, the warmest month Verileri (2010) and Kaya (2011). The region is surrounded by many mountains whose peaks are over 3000 meters high. High altitude, moisture-free sites are the most suitable for observatory construction, Koc-San et al. (2013).

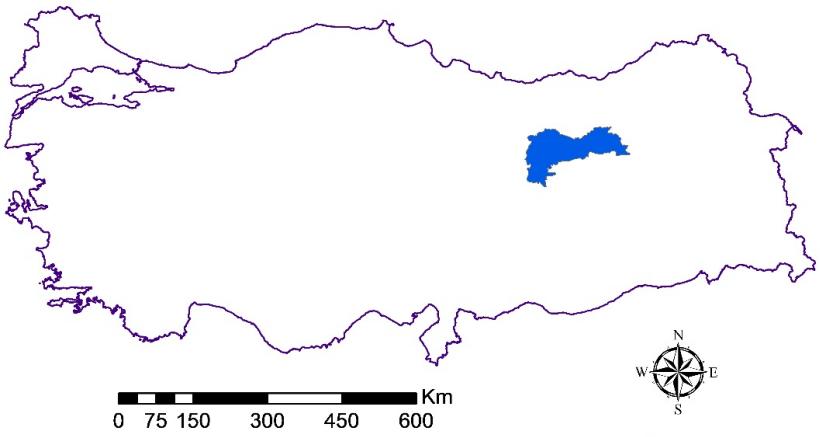

Figure 1. Location of the work area

In this study, datasets from three main areas (meteorology, geography and anthropogenes) were used to determine the most suitable location for astronomical observing conditions. The datasets are explained in detail.

2.1. Meteorological datasets

In our study, the meteorological data set consists of cloud cover, precipitable water, and wind speed parameters. One of the most important factors affecting

an astronomical observation is the cloud cover of the area to be observed, Jia et al. (2012). One of the most important criteria affecting atmospheric permeability is the amount of settable water. Cloud cover and precipitation water are the most important parameters in our study, Koc-San et al. (2013). Of the meteorological parameters, cloud cover and collapsing water data are products of Moderate Resolution Imaging Spectroradiometry (MODIS) data, which covers the entire Earth almost daily. MODIS data have resolutions of 250 m (2 bands) and 500 m (5 bands) in the VIS and SWIR bands, respectively, based on different methods, Barnes et al. (1998). In this study, the MOD10A1 products were used for cloud cover and MOD05L2 for stormwater. The MOD10A1 products were obtained from the National Snow and Ice Data Center (NSIDC) and the MOD05L2 products were obtained from the Atmosphere Archive and Distribution System (LAADS) (NASA-EOSDIS, 2022). The edge length of each MOD10A1/MYD10A1 granule is 1200 km (corresponding to about 10), and the projections are equidistant and sinusoidal. MOD10A1 provides a thematic map with HDF extension that includes data on snowpack fraction, snow, cloud mask, terrain, and water classes, Hall & Riggs (2007). MODIS cloud mask data is binary information about cloud cover, i.e., whether a cloud is present or not Strabala (2005). In this study, cloud cover data were obtained from the snow cover fraction layer of the MOD10A1 data, Hall & Riggs (2007). Sedimentable water content, another meteorological data set, is one of the important criteria affecting atmospheric permeability. Sensors have been developed to determine water vapor content (Advanced Very High-Resolution Radiometer (AVHRR), Sobrino et al. (2003), and MODIS, Gao & Goetz (1990) and Kaufman & Gao (1992). Another MODIS product, MOD05L2 (near-infrared and QA infrared), is used to determine water vapor content, Sobrino et al. (2003) and Kern et al. (2008). To obtain the map of the working area of water vapor, the infrared data sets of water vapor obtained from the MOD05L2 product were used to determine the water vapor content (NASA-EOSDIS, 2022). In this study, 4380 granules in HDF format were combined in the program GIS for the spatial information of each parameter cloud cover and precipitable water, and 1095 data in the study area were used (365 3 years), covering a 3-year period from January 1, 2020, to December 31, 2022. Wind speed data were obtained from the Global Wind Atlas 3.0 map, a free web-based application developed and operated by the Technical College of Denmark (DTU). The Global Wind Atlas 3.0 was published in collaboration with the World Bank Group using data provided by Vortex with funding from the Energy Sector Management Assistance Program (ESMAP) (more information: https://globalwindatlas). Our study used wind speed data from the GWA version 3.2 with a spatial resolution of 10 m to account for local variations in average wind speeds. The Global Wind Atlas (GWA) primarily supports wind energy development in the exploration phase and in the preliminary wind resource assessment phase prior to on-site meteorological surveys. The Global Wind Atlas provides wind source mapping at a horizontal grid of 250 m and wind source mapping at 10, 50, 100, 150, and 200

m above the ground level. Users can download GIS data for all layers at a point, in a specific area, or within a country. The speed at which air flows over the water surface affects the evaporation rate. Humidity depends on the amount of vapor in the air. Therefore, a higher wind speed results in minimal evaporation of water and lower humidity. Lower wind speed results in maximum evaporation of water and higher humidity, Ravi & D'Odorico (2005). Wind speed has an indirect effect on site selection for astronomical observatories.

2.2. Geographical datasets

Geographic Data Group; The Digital Elevation Model (DEM) consists of geology, landslides, active fault lines, and data. As altitude increases, sky transparency increases, Hudson & Simstad (2010), components that increase atmospheric scatter are reduced. Therefore, DEM is an important parameter. The Shuttle Radar Topography Mission (SRTM) has a spatial resolution of 90 m 90 m DEM represents the topography of the studied area. DEM Data used in the study were obtained from the USGS Earth Explorer. The data were processed in the ArcGIS 10.8 program, Bal et al. (2021). The construction areas of the buildings should be kept away from geological conditions, landslide zones, active fault lines, and floodplains. Considering that the building to be constructed is an observatory equipped with expensive equipment, it is important to choose the safest construction site. For this reason, maps of geology, landslides, and active fault lines were used in our study. Geology, landslide and active fault maps (for the study area) were drawn separately for each of the geology formation, landslide and active fault parameters using the drawing editor via the soil unit map viewer application of the General Directorate of Mineral Research and Exploration, Akbaş et al. (2011) and Üzer et al. (2013). In Erzincan province, it is divided into four basic tectonic-stratigraphic units of the pre-Eocene age, which have different environmental conditions and are tectonically connected. They are the Munzur Limestone, the Erzincan Nappe, the imen Mountain Nappe and the Kelkit-Rela autochthon from south to north. Of these nappes, the Kelkit autochthonous nappe lies on the imen Mountain nappe in the south and the Erzincan nappe in the north, and the imendaı nappe lies above the Erzincan nappe. The Munzur limestone napi is located below the Erzincan nappe, Yilmaz (1985). The data on the geological maps show that the rock classes of the study area are in seven different formations and are from the Cretaceous, Lower Miocene, Upper Miocene-Pliocene, Oligocene, Eocene, Miocene, Malm Cretaceous, Lower Cretaceous and Upper Cretaceous, Gürsoy (2012). Another criterion for selecting a suitable site is the landslide inventory data. Landslide maps from the General Directorate of Mineral Research and Exploration were used. According to the landslide maps, landslide activity consisted mainly of Miocene clastic neritic limestone, Mesozoic unconfined basic and ultrabasic rocks. In the landslide map prepared for the study area, all landslide activities were marked as areas unsuitable for construction. It is important to build as far as possible from

active fault lines, which is another parameter. The urban area is surrounded by the Northeast Anatolian Fault Line and the Ovacık Fault Line, as well as the secondary fault lines associated with these two main fault lines, Barka & Eyidoan (1993). Maps of active faults produced by the MTA were digitized using the GIS program, and maps of active fault lines were produced.

2.3. Anthropogenic datasets

Anthropogenic datasets were created using city lights, distance to roads, and point density of mine sites. City lighting is important for people to continue their activities when they cannot benefit from sunlight. It is one of the most important parameters that negatively affect astronomical observations. The Operational Line Scanning System (OLS) is one of the Defense Meteorological Satellite Program (DMSP) sensors and was originally developed for lunar light cloud observations, Elvidge et al. (1997). Its ability to image in low light has made it the preferred accurate and effective data source for imaging anthropogenic lights on the Earth's surface in cloudless night conditions without moonlight, Zhang & Seto (2011). In this study, the DMSP/OLS data were used to evaluate the effects of urban lights in selecting suitable locations. It is important to determine the positions of astronomical observatories in relation to mine sites because mine sites cause dustiness and affect sky opacity positively and sky observations negatively Koc-San et al. (2013). The locations of the mining sites were taken from the General Directorate of Mining Affairs of Turkey. In order to reduce the construction cost of the astronomical observatory and to make it easy to reach, the distance to the roads was used as a criterion in our study. These comparative data were obtained from the OpenStreetMap. The data for Turkey was obtained using the overpass turbo, Ma et al. (2015).

3. Methodology

In this study, there are five stages: (i) determining the criteria/factors and storing them in the environment GIS, (ii) data analysis, (iii) map evaluation using the MCDA method, (iv) determining the weight of each criterion using the AHP method and (v) combining the criteria. In this study, after analyzing raster data layers and digital data, a model was created in Arc- GIS 10.8 software. The data processing and analysis in this model is shown in the following analysis, Figure 2. In this study, three main parameters consisting of anthropogenic, meteorological, and geographic datasets were used to select the appropriate site, Koc-San et al. (2013). These datasets were obtained from the drawing editor, remote sensing data or digital maps, and a map was created for each dataset using the program GIS. It was ensured that the projection systems (WGS84) of the maps created or used were identical. Each data set used in this study is represented by a layer. Each data layer is converted from a raster layer to a vector layer. Many GIS -based applications are used to analyze these layers. A common field

was added to each layer, and the field values were set between 1 and 5, where 5 is the best score and 1 is the worst one. All data layers were converted from vector to raster again according to the generated field data. In the next step, the weights of each criterion were determined by pairwise comparisons of the experts' criteria (45 comparisons for 10 criteria), as required by the AHP model. Finally, the weighting values of each level were entered into the Weight Overly application in the GIS program and the most appropriate location within the boundaries of the study area was selected.

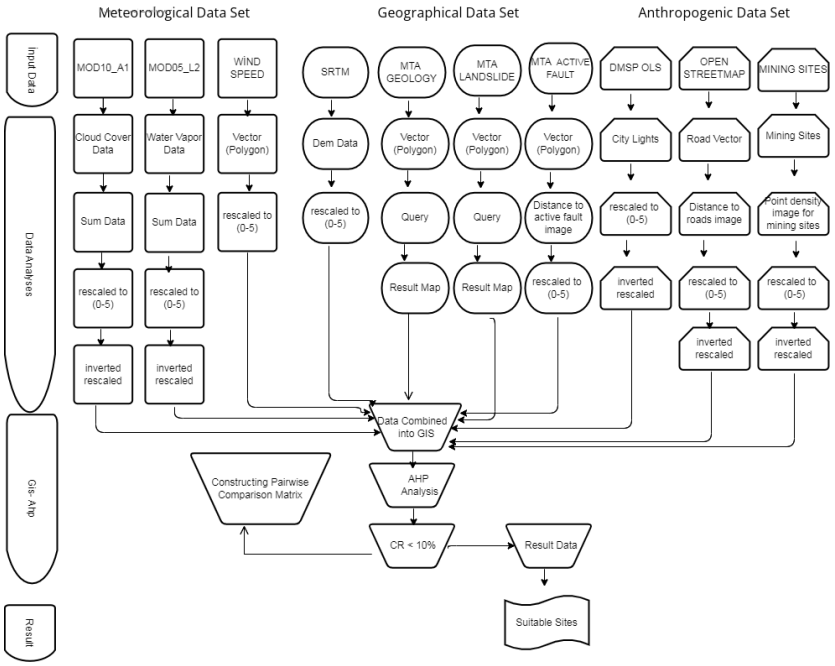

Figure 2. Flow chart of the process steps followed in the study.

3.1. Processing of meteorological data sets

3.1.1. Cloud cover data

Approximately 4380 granules were obtained from MOD10A1 between the years 2020 and 2022, from which 1095 data were obtained. These data were combined into a single layer. The obtained layer was used as spatial cloudiness data. Since areas with low cloud cover are considered ideal observation points, low pixel values with low cloud cover are scaled as 5 points and high pixel values with high cloud cover are scaled as 1 point (see Figure 3(a)). Cloud cover is directly

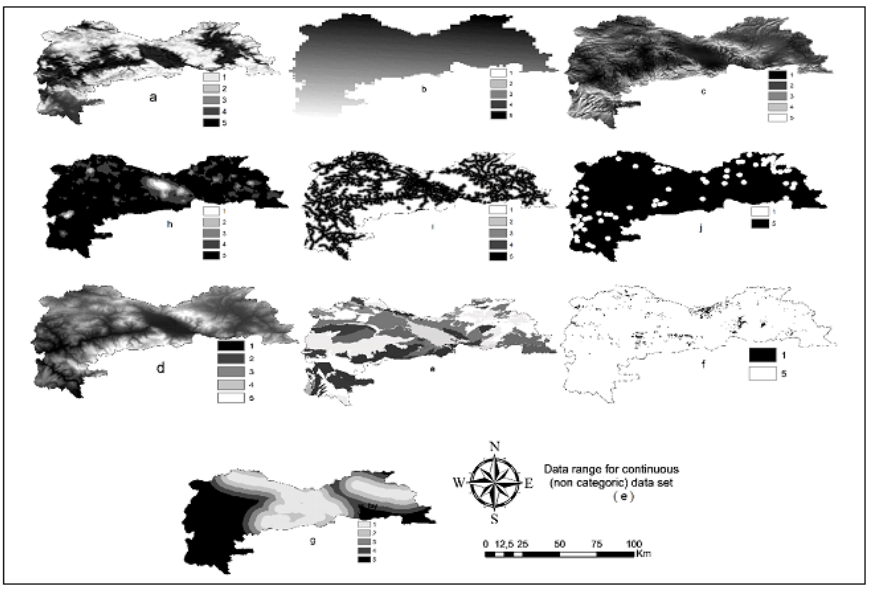

Figure 3. The data sets used; meteorological (cloud cover (a), rainy water (b)), wind speed (c)) geographical (DEM (d), geologically suitable areas (e), landslide (f), distance map of active fault lines (g)) and anthropogenic datasets (city lights (h), distance to roadmap (i) and point density (j) for mining operations).

effective in astronomical observations. The best observation conditions occur during periods of cloud-free weather (no clouds or very few clouds). According to the World Meteorological Organization, total cloud cover is defined as the part of the celestial dome covered by all visible clouds, Mekhaimr (2017). The celestial dome is divided into eight sections, each section is called an arrow, and an estimate is made on how many arrows the clouds cover. It is defined as clear weather or slightly cloudy ($<$ 2 octas), partly cloudy (3-5 octas) and cloudy sky ($\geq$ 6 octas), Mekhaimr (2017). Observation conditions according to cloud cover classifications, 2 octas and below are the most ideal conditions for outdoor observation, the 3-5 octas December is defined as partly cloudy skies and partly offers periods of observation. Between the years 2010-2022, the cloud closure data of the meteorological department of Erzincan province were interpreted according to the above-mentioned octa data classes, and the number of days that can be observed was estimated as 247.5 days per year.

3.1.2. Precipitable water data

Rainfall information was obtained from the MOD05L2 dataset using the water vapor infrared data channel. For the three-year period, the settable water

infrared data were processed and converted into a single data layer using the program GIS, and the stormwater data were presented using this layer. The stormwater vapor data are scaled from 1 to 5. In the scaling, 1 represents more settleable water vapor and 5 represents less settleable water vapor (Figure 3(b)).

3.1.3. Wind speed data

Wind speed data are from the Global Wind Atlas database. The data have a spatial resolution of 250 m. The data for Turkey obtained from the Global Wind Atlas are arranged according to the boundaries of the study area. The wind speed data are scaled from 1 to 5. Regions with low wind speeds were scored as 1 and regions with high wind speeds were scored as 5 (Figure 3 (c)).

3.2. Processing of geographic datasets

3.2.1. Geology data

In the study, the geological map of the study area was created in a geojson format using the drawing editor application from the content of the geoscientific map viewer of the General Directorate of Mineral Research and Exploration. The obtained map was digitized using the program GIS and used as a geological data layer. Alluvial fans, sand, dunes and debris cones are marked on the map as unsuitable areas for the construction site, while the other geological infrastructures are marked on the map as suitable areas. In this data layer, a value of 5 represents geologically suitable areas and a value of 1 represents unsuitable areas (Figure 3 (e)), Koc-San et al. (2013).

3.2.2. Landslide inventory data

The layer of landslides was created by the same processes as the layer of geology. There are many active landslides in the study area. Areas with landslides should be excluded when selecting a suitable site Koc-San et al. (2013). During the study, landslide-prone and landslide-free areas were scaled as 1 and 5, respectively (Figure 3 (f)).

3.2.3. Active fault lines data

In this study, active fault lines were identified as vectors using the geoscientific map viewer of the General Directorate of Mineral Research and Exploration. These vectors were converted to raster data, and locations 20000 m and farther from the fault lines were scaled as 5, and locations 5000 m and farther were scaled as 1. The distance map produced was used as active fault line data (Figure 3 (g)).

3.2.4. Digital elevation model

During the study, GTOPO30 data was used for the elevation information, two granules with the boundaries of Turkey were downloaded, these two granules were combined in the application GIS and the study area was cut out from the map. The data range in the study area is between 755 and 3412 m. Accordingly, these data were divided into five data groups on a scale of 1 to 5, with the highest points scaled as 5 and the lowest as 1. (Figure 3 (d)).

3.3. Processing of anthropogenic datasets

3.3.1. City lights data

Data from the Defense Meteorological Satellite Program (DMSP) Operational Linescan System (OLS) databases within the study area boundaries were used Elvidge et al. (2001). The data have a radiometric resolution of 32 bits. The data sets are scaled from 1 to 5. 1 represents the most illuminated areas, while 5 represents the least illuminated areas (Figure 3 (h)).

3.3.2. Mining activities data

The study area includes chrome, iron, manganese, copper-zinc-lead metal mines and industrial raw materials such as asbestos, barite, gypsum, magnesite, marble, perlite, bricks and sulfur. The dust layer around mining operations affects astronomical observations. For this reason, a grid map has been created to define mining areas. The regions where mining is carried out are divided into 5 scales in the range of 500-2000 m and above. Distances of 2000 m and more to mining sites are scaled by a value of 5, 500 m and less by a value of 1 (Figure 3(j)).

3.3.3. Road information data

Road proximity data were obtained from the OpenStreetMap application. The obtained data were converted from raster to vector data, and the road proximity parameters were defined and converted to raster data again. The raster data are divided into the distance ranges of 100 m and less and 500 m and more. Distances of 100 m and less are scaled by a value of 5, and distances of 500 m and more are scaled by a value of 1 (Figure 3(i)).

3.4. Analytic hierarchy process

The maps created for each of the 10 data in a raster data format were scaled between 1 and 5 and combined with the program GIS according to the weight ratios determined by the AHP method. The AHP method is based on comparing data layers with each other by numerical evaluation on an absolute number scale, Saaty (1980), and is a good way to address seemingly complex problems with a

simple hierarchy, Cheng et al. (1999). While the individual criteria in the AHP are compared with each other, their importance levels are evaluated using odd numbers between 1 and 9, although even numbers may be preferred in cases where the determinant is ambiguous. The assigned criteria values appear in the AHP matrix (see tab. 1). The importance of the criteria was determined by expert decision-makers in the fields of astronomical observations, earth sciences, meteorology, and urban planning. When comparing the two criteria, the most important criterion determined by the experts was rated 9. It is rated 1 if the two criteria are equally important.

Table 1. A pairwise comparison scale based on Saaty's Fundamental Scale (Triantaphyllou et al. (1995))

Intensity of Importance	Definition	Explanation
1	Equal importance	Two activities contribute equally to the objective
2	Weak or slight	
3	Moderate importance	Experience and judgement strongly favor one activity over another
4	Moderate plus	
5	Strong importance	Experience and judgement strongly favor one activity over another
6	Strong plus	
7	Very strong or demonstrated importance	An activity is favored very strongly over another; its dominance demonstrated in practice
8	Very, very strong	
9	Extreme importance	The evidence favoring one activity over another is of the highest possible order of affirmation

The specific AHP procedures are:

1. Determining the importance relationship between the indices and creating the overall AHP structure.

2. Creating the following comparison matrix A with the weights determined by the experts based on the scale from 1 to 9 (see tab. 2), Saaty (1990),

$$A = \begin{pmatrix} a_{11} & a_{12} & ... & a_{1n} \\ a_{21} & a_{22} & ... & a_{2n} \\ . & . & ... & . \\ a_{m1} & a_{m2} & ... & a_{mn} \end{pmatrix} \tag{1}$$

where a_{mn} is the result of comparing the m'th factor with its importance relative to the nth factor, $a_{mn} > 0$, $a_{mn} = 1/a_{nm}$, $a_{mn} = 1$ (when $m = n$).

3. A is the comparison matrix, W and $w_i (i = 1, 2, ..., n)$ represent the corresponding eigenvector of λ_{max} and the weighting value for ranking, respectively and λ_{max} represents the largest eigenvalue of the matrix; in this study, the λ_{max} value was determined to be 10.911.

$$\begin{pmatrix} a_{11} & a_{12} & ... & a_{1n} \\ a_{21} & a_{22} & ... & a_{2n} \\ . & . & ... & . \\ a_{m1} & a_{m2} & ... & a_{mn} \end{pmatrix} \times \begin{pmatrix} w_1 \\ w_2 \\ ... \\ w_i \end{pmatrix} \tag{2}$$

$$\lambda_{max} = \frac{1}{n} \sum_{w_i}^{n} \frac{A_i . W_i}{W_i} \tag{3}$$

4. The consistency of the pairwise comparison matrix should be checked using the consistency index (C.I). The consistency check is performed (C.I, Equation 4). In this study, the C.I value was calculated as 0.107,

$$C.I = \frac{\lambda_{max} - 1}{n - 1}, \tag{4}$$

In addition, to check the consistency of the created matrix, Saaty (1980), the consistency ratio (C.R) value should be determined. The C.R formula is shown below,

$$C.R = \frac{C.I}{R.I}, \tag{5}$$

Where C.I is the consistency index and R.I is the random inconsistency, Saaty et al. (2008) and Saaty & Tran (2007). The critical value for the C.R value is 0.10. Values above this value are considered inconsistent, while values below this value are considered consistent, Saaty et al. (2008), Saaty & Tran (2007) and Koc-San et al. (2013). For n = 10, the value of the random

Table 2. The AHP pairwise comparison matrix and calculated weights.

	A	B	C	D	E	F	G	H	I	J
A	1	0.333	0.2	0.333	0.200	0.143	0.143	0.125	0.111	0.125
B	3	1	1	0.333	0.333	0.333	0.143	0.125	0.111	0.167
C	5	1	1	0.333	0.333	0.333	0.143	0.125	0.111	0.167
D	3	3	3	1	0.250	0.333	0.143	0.125	0.111	0.200
E	5	3	3	4	1	1	0.167	0.143	0.125	0.333
F	7	3	3	3	1	1	0.333	0.333	0.200	0.500
G	7	7	7	7	6	3	1	1	0.333	0.500
H	8	8	8	8	7	3	1	1	0.333	1
I	9	9	9	9	8	5	3	3	1	1
J	8	6	6	5	3	2	2	1	1	1

discrepancy is R.I=1.49, Saaty & Tran (2007). In our study, the C.R value was calculated as 0.068. The matrix obtained by the experts through pairwise comparisons (see tab. 2) is consistent and can be used in the analysis phase.

$\lambda_{max} = 10.911$, C.I = 0.107, R.I (n = 10) = 1.49, C.R = 0.068 (A: distance to roads, B: geology, C: landslide, D: distance to active faults, E: wind speed F: point density of mining sites, G: city lights, H: rainy water, I: cloud cover and J: DEM).

The 10 maps with data layers used in the study were overlaid in the program GIS in relation to the weighting ratios determined by the AHP method, and the most suitable areas (Figure 4, red areas) were proposed for the construction of the astronomical observatory.

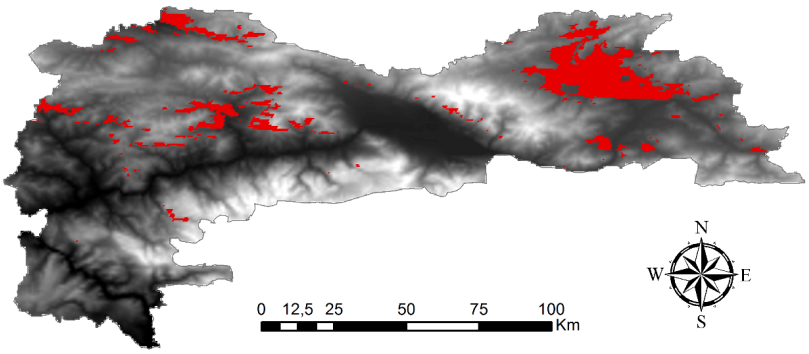

Figure 4. Map of candidate sites for the astronomical observatory covered with DEM (marked in red)).

4. Results and discussions

The most suitable site within the study area was determined by multiplying and overlaying each of the criteria maps (10 maps) obtained after the steps described above with the criteria weights calculated using AHP (Figure 4). The three main criteria identified, meteorological, geographic, and anthropogenic, are shown in red in the most suitable areas (Figure 4) In this study, according to experts, the most important parameters are meteorological datasets that contain information about cloud cover and precipitation water. 3-year image data (between 2020-2022) of these datasets were analyzed. Dealing with over 2000 images provides reliable information in the spatial domain, Koc-San et al. (2013). The 3-year meteorological dataset provides information reliability about the current meteorological condition of the study area and minimizes meteorological changes due to global warming. Statistically, 3 years of data (1095 data from the combination of 4380 granules) is satisfactory for this type of analysis, Koc-San et al. (2013).

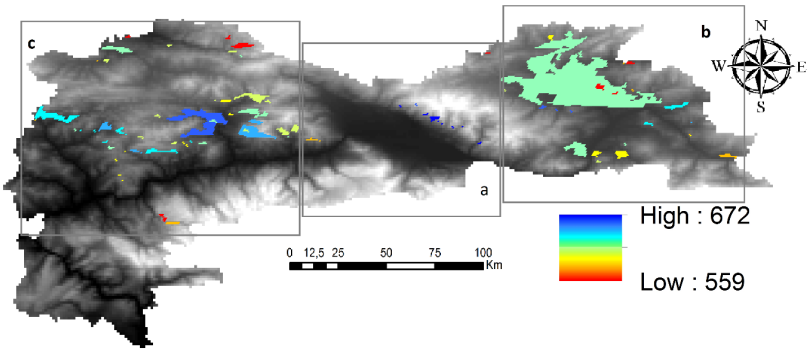

Figure 5. The number of cloud-free days obtained as a result of the 3-year data analysis.

As a result of the analysis of 3-year cloud cover data, the maximum and minimum values of the number of cloud-free days in the study area are shown in Figure 5. The map showing the number of cloud-free days was formed as a, b, c (see Figure 5). Among these classes, the highest number of cloud-free days was determined in the pixels in class a (598-672 days) (see Figure 6, blue pixels). The lowest number of days (559-632 days) was observed in pixels in class c. Although the pixels in class a are ideal for the number of cloud-free days, they are the candidate regions closest to the city center and the university campus. The closest candidate pixel to the city center is at least 8.39 km.

Precipitation water and water vapor is an effective parameter especially for astronomical observatories where observation activities are carried out at in-

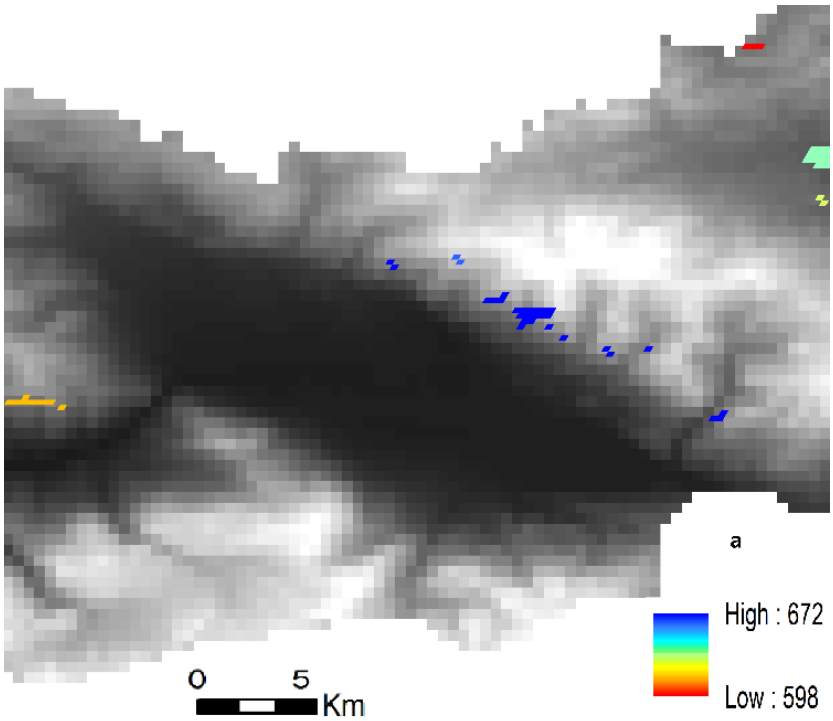

Figure 6. Maps of regions and the number of cloud-free days within the provincial borders of Erzincan.

frared wavelengths. Pérez-Jordán et al. (2015). As the water vapor gets closer to the earth, its relationship with the humidity value increases. Observations are not carried out when the humidity value exceeds 85% Solmaz et al. (2021). The annual average humidity of Erzincan Province was 64.26%, Kaya (2011). These average humidity values mean that observations can be made in general.

The smallest and maximum wind speed values within the provincial borders of Erzincan are shown in Figure 7. Wind speed is the limit value for 11 m/s observations, Solmaz et al. (2021). There are very few areas above the limit value within the provincial borders of Erzincan. However, wind speed values above the limit value are not among the candidate pixels (see Figure 7, red).

5. Conclusion and Recommendations

This study presents an exemplary application of the approach created by using MCDA, remote sensing and GIS technologies in selecting the most suitable site for the astronomical observatory as a result of analyzing complex criteria. This

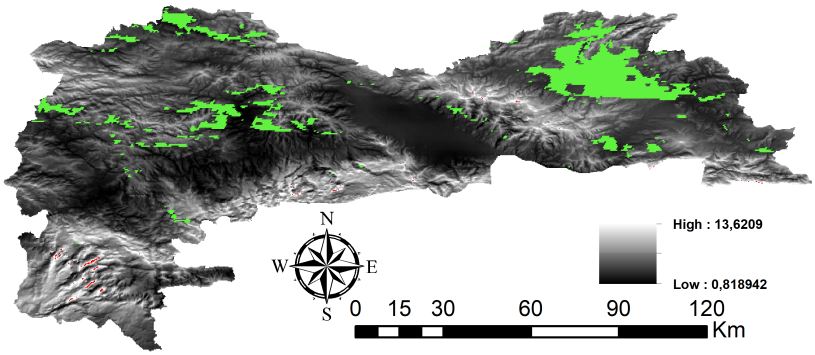

Figure 7. Candidate areas (green) and areas with wind speeds greater than 11m/s (red) on the wind speed map.)

approach is a powerful method for site locating an astronomical observatory. This methodology, supported by field trials, will provide temporal, economic, and energy advantages in determining the location of the observatory. Applicable for areas where the future observatory construction is planned.

Acknowledgements. I would like to thank the experts who contributed to the creation of the decision matrix of the AHP method.

References

Akbaş, B., Akdeniz, N., Aksay, A., et al., 1: 1.250. 000 Ölçekli Türkiye Jeoloji Haritası. 2011, *Maden Tetkik ve Arama Genel Müdürlüğü Yayını, Ankara-Türkiye*

Aman, D. D. & Aytac, G., Multi-criteria decision making for city-scale infrastructure of post-earthquake assembly areas: Case study of Istanbul. 2022, *International Journal of Disaster Risk Reduction*, **67**, 102668

Bal, M., Dandpat, A. K., & Naik, B., Hydrological modeling with respect to impact of land-use and land-cover change on the runoff dynamics in Budhabalanga river basing using ArcGIS and SWAT model. 2021, *Remote Sensing Applications: Society and Environment*, **23**, 100527

Barka, A. & Eyidoan, H., The Erzincan earthquake of 13 March 1992 in eastern Turkey. 1993, *Terra Nova*, **5**, 190

Barnes, W. L., Pagano, T. S., & Salomonson, V. V., Prelaunch characteristics of the moderate resolution imaging spectroradiometer (MODIS) on EOS-AM1. 1998, *IEEE Transactions on Geoscience and Remote Sensing*, **36**, 1088

Bilgilioglu, S. S., Gezgin, C., Orhan, O., & Karakus, P., A GIS-based multi-criteria decision-making method for the selection of potential municipal solid waste disposal

sites in Mersin, Turkey. 2022, *Environmental Science and Pollution Research*, **29**, 5313

Cheng, C.-H., Yang, K.-L., & Hwang, C.-L., Evaluating attack helicopters by AHP based on linguistic variable weight. 1999, *European journal of operational research*, **116**, 423

Cowles, K., Site selection criteria for the optical atmospheric visibility monitoring telescopes. 1989, *The Telecommunications and Data Acquisition Report*

Elvidge, C. D., Baugh, K. E., Kihn, E. A., Kroehl, H. W., & Davis, E. R., Mapping city lights with nighttime data from the DMSP Operational Linescan System. 1997, *Photogrammetric Engineering and Remote Sensing*, **63**, 727

Elvidge, C. D., Imhoff, M. L., Baugh, K. E., et al., Night-time lights of the world: 1994–1995. 2001, *ISPRS Journal of Photogrammetry and Remote Sensing*, **56**, 81

Gao, B.-C. & Goetz, A. F., Column atmospheric water vapor and vegetation liquid water retrievals from airborne imaging spectrometer data. 1990, *Journal of Geophysical Research: Atmospheres*, **95**, 3549

Gürsoy, Ö. 2012, Cndaki (erzincan Sivas-koyulhisar Arası) Litolojik Farklılık Ve Benzerliklerin Uzaktan Algılama Yöntemleri İle Belirlenmesi, PhD thesis, Fen Bilimleri Enstitüsü

Hall, D. K. & Riggs, G. A., Accuracy assessment of the MODIS snow products. 2007, *Hydrological Processes: An International Journal*, **21**, 1534

Hudson, K. & Simstad, T., The share astronomy guide to observatory site selection. 2010, *Neal Street Design Inc*, **1**

Jia, Y., Yong-qiang, Y., Hong-shuai, W., et al., Processing method of night-time cloudiness for astronomical site selection. 2012, *Chinese Astronomy and Astrophysics*, **36**, 457

Kaufman, Y. J. & Gao, B.-C., Remote sensing of water vapor in the near IR from EOS/MODIS. 1992, *IEEE Transactions on Geoscience and Remote Sensing*, **30**, 871

Kaya, M., Erzincan iklim ve meteoroloji verileri. 2011, *Tesisat Mühendisliği Dergisi*, **34**, 42

Kern, A., Bartholy, J., Borbás, É. E., et al., Estimation of vertically integrated water vapor in Hungary using MODIS imagery. 2008, *Advances in space research*, **41**, 1933

Koc-San, D., San, B., Bakis, V., Helvaci, M., & Eker, Z., Multi-Criteria Decision Analysis integrated with GIS and remote sensing for astronomical observatory site selection in Antalya province, Turkey. 2013, *Advances in Space Research*, **52**, 39

Ma, D., Sandberg, M., & Jiang, B., Characterizing the heterogeneity of the OpenStreetMap data and community. 2015, *ISPRS International Journal of Geo-Information*, **4**, 535

Mekhaimr, S. A., Atmospheric conditions affecting seeing at St. Catherine: Estimation of operational time for NRIAG new telescope. 2017, *NRIAG Journal of Astronomy and Geophysics*, **6**, 5

Pérez-Jordán, G., Castro-Almazán, J., Muñoz-Tuñón, C., Codina, B., & Vernin, J., Forecasting the precipitable water vapour content: validation for astronomical observatories using radiosoundings. 2015, *Monthly Notices of the Royal Astronomical Society*, **452**, 1992

Ravi, S. & D'Odorico, P., A field-scale analysis of the dependence of wind erosion threshold velocity on air humidity. 2005, *Geophysical Research Letters*, **32**

Saaty, T., The analytic hierarchy process (AHP) for decision making. 1980, in *Kobe, Japan*, 1–69

Saaty, T. L., What is the analytic hierarchy process? Mathematical models for decision support. 1988, *NATO ASI Series*, **48**, 109

Saaty, T. L., How to make a decision: the analytic hierarchy process. 1990, *European journal of operational research*, **48**, 9

Saaty, T. L. & Tran, L. T., On the invalidity of fuzzifying numerical judgments in the Analytic Hierarchy Process. 2007, *Mathematical and Computer Modelling*, **46**, 962

Saaty, T. L. et al., Decision making with the analytic hierarchy process. 2008, *International journal of services sciences*, **1**, 83

Sobrino, J., El Kharraz, J., & Li, Z.-L., Surface temperature and water vapour retrieval from MODIS data. 2003, *International Journal of Remote Sensing*, **24**, 5161

Solmaz, A., Aksaker, N., Akyüz, A., et al., ÇÜ Uzay Bilimleri ve Güneş Enerjisi Araştırma ve Uygulama Merkezi (UZAYMER): I. Gözlem Koşulları ve Güncel Projeler. 2021, *Turkish Journal of Astronomy and Astrophysics*, **2**, 1

Strabala, K. I. 2005, *MODIS cloud mask user's guide* (University of Wisconsin–Madison)

Triantaphyllou, E., Mann, S. H., et al., Using the analytic hierarchy process for decision making in engineering applications: some challenges. 1995, *International journal of industrial engineering: applications and practice*, **2**, 35

Tulun, Ş., Arsu, T., & Gürbüz, E., Selection of the most suitable biogas facility location with the geographical information system and multi-criteria decision-making methods: a case study of Konya Closed Basin, Turkey. 2022, *Biomass Conversion and Biorefinery*, 1

Üzer, M., Emre, Ö., Duman, T. Y., et al. 2013, *Açıklamalı Türkiye Diri Fay Haritası, Ölçek 1: 1.250. 000* (Maden Tetkik ve Arama Genel Müdürlüğü)

Verileri, E. İ. U. Y. M., Çevre ve Orman Bakanlığı. 2010, *Devlet Meteoroloji İşleri Genel Müdürlüğü*

Walker, M. F., High quality astronomical sites around the world. 1984, in European Southern Observatory Conference and Workshop Proceedings, Vol. **18**, *European Southern Observatory Conference and Workshop Proceedings*, 3–21

Yilmaz, A., Yukari Kelkit cayi ile Munzur daglari arasinin temel jeoloji özellikleri ve yapisal evrimi. 1985, *Türk jeoloji Kurumu Bülteni*, **28**, 79

Zhang, Q. & Seto, K. C., Mapping urbanization dynamics at regional and global scales using multi-temporal DMSP/OLS nighttime light data. 2011, *Remote Sensing of Environment*, **115**, 2320